AIP Advances

Pressure-induced phase transitions of ZnSe under different pressure environments

Cite as: AIP Advances **9**, 025004 (2019); https://doi.org/10.1063/1.5082209
Submitted: 19 November 2018 . Accepted: 25 January 2019 . Published Online: 06 February 2019

Chang Pu, Lidong Dai, Heping Li, Haiying Hu, Kaixiang Liu, Linfei Yang, and Meiling Hong

Pressure-induced phase transitions of ZnSe under different pressure environments

Cite as: AIP Advances 9, 025004 (2019); doi: 10.1063/1.5082209
Submitted: 19 November 2018 • Accepted: 25 January 2019 •
Published Online: 6 February 2019

Chang Pu,[1,2] Lidong Dai,[1,a)] Heping Li,[1] Haiying Hu,[1] Kaixiang Liu,[1,2] Linfei Yang,[1,2] and Meiling Hong[1,2]

AFFILIATIONS

[1] Key Laboratory of High Temperature and High Pressure Study of the Earth's Interior, Institute of Geochemistry, Chinese Academy of Sciences, Guiyang, Guizhou 550081, China

[2] University of Chinese Academy of Sciences, Beijing 100039, China

[a)] **Author to whom correspondence should be addressed:** dailidong@gyig.ac.cn

ABSTRACT

The structural, vibrational and electronic properties of ZnSe under different pressure environments up to ~40.0 GPa were investigated using a diamond anvil cell in conjunction with ac impedance spectroscopy, Raman spectroscopy and high-resolution transmission electron microscopy. Under the non-hydrostatic condition, ZnSe exhibited a structural phase transition from a zinc-blende to a cinnabar structure at ~4.9 GPa, indicated by the obvious splitting of the transverse optical mode in the Raman spectra and a noticeable variation in the slope of the electrical conductivity. With increasing pressure, metallization appeared at ~12.5 GPa, which was characterized by the high-pressure Raman spectroscopy and temperature-dependent electrical conductivity results. When the pressure was increased up to ~30.0 GPa, another phase transition was identified by the appearance of a new peak in the Raman spectra. Compared to the non-hydrostatic condition, a roughly 2.0 GPa delay of transition pressure for ZnSe was observed at the hydrostatic condition. However, the structural phase transformation was found to be irreversible only under the non-hydrostatic condition. The unique properties displayed by ZnSe under different pressure environments may be attributed to the constrained interlayer interaction owing to the presence of the pressure medium.

I. INTRODUCTION

The pressure-induced phase transitions for some ZnX (X=O, S, Se and Te) types of semiconductors have become a fundamental topic in condensed matter physics owing to their extensive applications in the fields of optoelectronic devices.[1–5] Zinc selenide (ZnSe) is a typical semiconductor with a direct band gap, and crystallizes into a zinc-blende (ZB) structure at ambient conditions. It has attracted great interest because of its wide use in the blue-light-emitting diodes and quantum-well devices.[6] A systematic study of the high-pressure behaviors of ZnSe would be helpful to further understand the pressure-induced variations of the crystalline and electrical properties for ZnX-type materials and promote its industrial production.

The pressure-induced phase stability of ZnSe has been previously investigated by Raman spectroscopy, X-ray diffraction and electrical resistivity experiments.[7–13] However, some dispute exists regarding the structural and vibrational properties of ZnSe, as well as the transition points at high pressures. Some researchers have observed a splitting phenomenon of the transverse optical (TO) mode in Raman spectroscopy at 4.7 GPa, and have thus suggested the occurrence of a phase transition for ZnSe from the zinc-blende to the cinnabar phase at 4.7 GPa.[7] More recently, Yao *et al.* have investigated this phase transition by Raman spectroscopy and angular dispersive X-ray diffraction up to 32 GPa under the hydrostatic condition. A similar splitting phenomenon for the TO mode in the Raman spectra and a discontinuous variation in the relative volume with pressure was observed at 5.5 GPa, and their results also indicated an occurrence of a phase transition for ZnSe.[8] In contrast, other researchers have not observed any discontinuous variations for the TO mode in the slope of the pressure dependence of Raman shifts up

to 5.5 GPa.[9] At higher pressures, Greene *et al.* have reported that ZnSe directly transforms from a zinc–blende (ZB) to a distorted rock–salt (RS) state at ~11.8 GPa, as indicated by high pressure X–ray diffraction experiments.[10] Itkin *et al.* have investigated the high pressure electrical property of ZnSe at 0–20 GPa using temperature–dependent electrical resistivity experiments, and further confirmed that ZnSe undergoes a metallization process from a semiconducting four–fold coordinated ZB structure to a six–fold coordinated metallic rock structure at pressures higher than 13.5 GPa.[11] In addition to these experimental results, some theoretical calculation studies of the high pressure phase stability of ZnSe have been reported, and also remain controversial. For instance, Durandurdu reported that the ZB–RS phase transition for ZnSe occurs at 10.8 GPa.[14] With increasing pressure, another phase transition of ZnSe from an RS to an orthorhombic (Cmcm) structure was obtained by Cote *et al.* at ~36.0 GPa.[15] However, Cui *et al.* have reported the RS–Cmcm phase transition to occur at ~29.8 GPa.[16]

It is well known that the electrical properties of some semiconductors are sensitive to the degree of hydrostatic conditions.[1] For instance, molybdenum disulfide was found to undergo a pressure–induced permanent metallization only under non–hydrostatic conditions.[17] The ZB–RS phase transition of ZnSe at high pressure is reversible under hydrostatic or quasi–hydrostatic conditions on the basis of previous Raman scattering and electrical resistivity experiments at the pressure ranges of 0–36.0 GPa, whereas the transitions for ZnSe before and after compression under non–hydrostatic conditions are unknown.[8,13] As a representative layered semiconductor material, there are no experimental reports of phase changes in ZnSe as a function of pressure medium.

In this study, we report three phase transitions for ZnSe under both non–hydrostatic and hydrostatic conditions at pressures up to ~40.0 GPa using a diamond anvil cell (DAC) in conjunction with impedance spectroscopy, Raman spectroscopy and high resolution transmission electron microscopy (HRTEM). Selected area electron diffraction patterns by HRTEM analysis are obtained for the recovered sample after decompression to further disclose whether it is isostructural with the initial ZnSe phase. In addition, the high pressure phase stability of ZnSe under different pressure environments is discussed in detail.

II. EXPERIMENTAL

A high–purity ZnSe powder sample (99.999%; Leshan Kai Yada Technology Co., Ltd., Sichuan Province, China) was used herein. High pressure was generated in a diamond anvil cell with an anvil culet of 300 μm in diameter. In the Raman scattering experiments, a single ruby crystal was added into the sample chamber to calibrate the pressure on the basis of the wave number shift of the fluorescence band of the trivalent chromic ion. Helium was adopted as a pressure medium to provide the hydrostatic condition, and no pressure medium was used for the non–hydrostatic condition. To measure the uniaxial stress of the sample at the pressure range 1.3–42.2 GPa under the non–hydrostatic condition, several small rubies were placed in the center and at the edge of the sample chamber. The Raman spectra were collected by a Raman spectrometer (Invia, Renishaw) equipped with a confocal microscope (TCS SP8, Leica) and a CCD camera (Olympus). The typical excitation laser power used herein was ~20 mW for Raman spectroscopy and 0.5–40 μW for fluorescence spectroscopy, achieved using a 514.5 nm argon ion laser (Spectra Physics) as the excitation light source (power <1 mW). With a spectral resolution of 1.0 cm^{-1}, the Raman spectra were collected in the range of 100–600 cm^{-1}. Some available high–pressure overlapping Raman band locations were determined using a Lorenz–type fitting function in the PeakFit software. The microstructure and interlayer space of the recovered sample were observed using transmission electron microscopy (TEM; Tecnai G2 F20 S–TWIN TMP).

High pressure electrical conductivity experiments were conducted in a DAC possessing a 300 μm–diameter anvil culet. First, the sample was crushed into powder (~30 μm–diameter particles). Next, a T–301 stainless steel gasket was pre–indented to a thickness of ~40 μm and a hole 200 μm in diameter was created with a laser. A mixture of boron nitride powder and epoxy resin was then crushed into the hole, and another hole 100 μm in diameter was drilled to form an insulating sample chamber. The ac impedance spectroscopy was performed with an impedance spectrometer (1260, Solartron) with a dielectric interface (1296, Solartron) at frequencies of 10^{-1}–10^{7} Hz. Further, a plate electrode was integrated between the upper and lower diamond anvils, and a K–type thermocouple with an estimated accuracy of 5 K was directly bonded to one side of the diamond anvil for temperature measurements. All of the Raman scattering and electrical conductivity measurements for ZnSe were conducted at least three times under non–hydrostatic conditions. Detailed descriptions of the experimental procedure can be found elsewhere.[18,19]

III. RESULTS AND DISCUSSION

To determine the pressure–induced phase transitions of ZnSe, a series of Raman spectra at pressures up to ~40.0 GPa and room temperature under both non–hydrostatic and hydrostatic conditions were conducted. The Raman spectra and corresponding experimental results during compression and decompression under the non–hydrostatic condition are shown in Fig. 1. At 0.3 GPa, two prominent Raman peaks attributed to the transverse optical (TO) and the longitudinal optical (LO) phonon modes were observed at 204.9 and 251.6 cm^{-1}, respectively, which was in good agreement with previous studies.[10,20] With increasing pressure, both the TO and LO peaks shifted to higher wave numbers and weakened in intensity. At 4.9 GPa, two corresponding peaks were formed by splitting of the TO peak, which may be owing to a phase transition from a zinc–blende to a cinnabar structure.[7] The split peak at 180.9 cm^{-1} was induced by mode softening, and exhibited a red shift at pressures less than 12.5 GPa and then moved to higher wave numbers with increasing pressure.

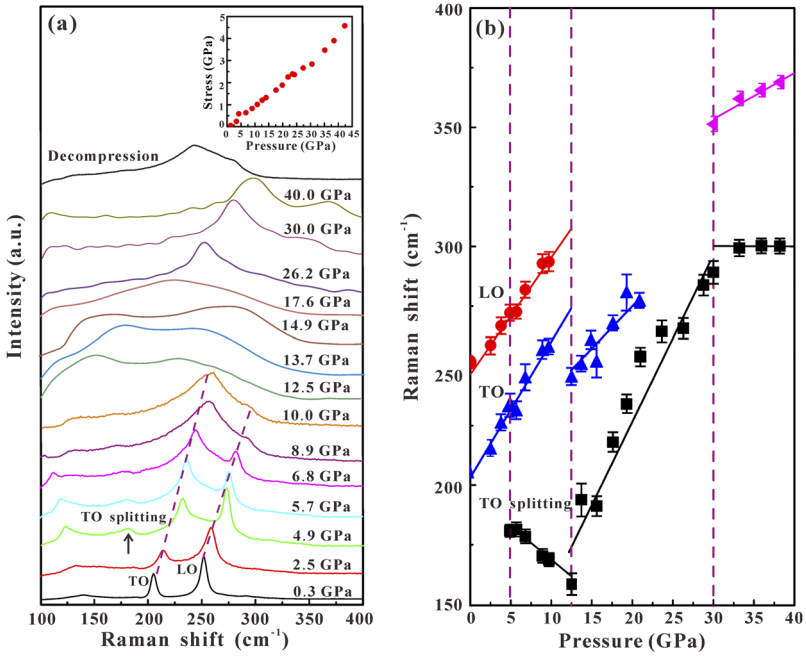

FIG. 1. (a) Raman spectra of ZnSe at the pressure range of 0.3–40.0 GPa and room temperature under the non–hydrostatic condition. Inset: the positive relevance between pressure and the uniaxial stress. (b) Raman shift of ZnSe with increasing pressure. TO: transverse optical mode and LO: longitudinal optical mode.

At the pressure of 12.5 GPa, the LO peak disappeared, indicating a transition of the ZnSe semiconductor to the metal phase, as reported by previous Raman scattering results at the hydrostatic condition.[7,8] At 30.0 GPa, one clear new peak appeared at 351.2 cm^{-1} and became stronger with increasing pressure. When the pressure was removed, however, the spectrum was not completely recovered and the LO phonon mode was still not evident. Figure 1(b) shows the linear relationship between pressure and the Raman shift, wherein the TO and LO modes both exhibited blue shifts with increasing pressure. When the pressure was enhanced up to 12.5 GPa, the LO phonon mode disappeared and the pressure–dependent variations of the TO and TO splitting modes exhibited an inflection point, respectively. At 30.0 GPa, one new vibrational mode appeared and a discontinuous variation of the TO splitting mode was observed. Table I presents the detailed pressure dependence of the Raman shifts and the corresponding fitting parameters for ZnSe under the non–hydrostatic condition.

Under the hydrostatic condition, some similar variations were observed in the Figs. 2(a) and 2(b) at pressures up to 39.0 GPa and at room temperature. It can be seen that the TO (204.7 cm^{-1}) and LO (251.6 cm^{-1}) phonon peaks shifted to higher wave numbers with increasing pressure, and a splitting of the TO peak occurred at 6.7 GPa. Further, the LO peak disappeared at the pressure 14.1 GPa. At pressures higher than 34.2 GPa, one new peak at 340.86 cm^{-1} can be clearly observed in the Raman spectrum of ZnSe. Upon decompression, the Raman spectrum of ZnSe was completely recoverable to its original state. In Fig. 2(b), the variations of the Raman shift with increasing pressure for the three primary modes revealed three critical points (6.7, 14.1 and 34.2 GPa) under the hydrostatic condition. It can be seen that the TO splitting mode appeared at 6.7 GPa, and exhibited two clearly discontinuous points at 14.1 and 34.2 GPa in the slope of the pressure–dependent Raman shift. The LO and TO modes shifted continuously with pressure but disappeared at 14.1 GPa. When the pressure was increased to 34.2 GPa, one new Raman mode appeared and monotonically shifted to higher wave numbers with pressures. Table II presents the detailed pressure dependence of the Raman shifts and the corresponding fitting parameters for ZnSe under the hydrostatic condition.

TABLE I. Pressure dependence of the Raman shifts for ZnSe under the non–hydrostatic condition. The values of mode frequencies ω (P_0) (cm^{-1}), pressure P (GPa), and pressure dependence $d\omega/dP$ ($cm^{-1}GPa^{-1}$) were extrapolated. TO: transverse optical mode and LO: longitudinal optical mode.

Mode	ω (P_0)	$d\omega/dP$<12.5 GPa	12.5 GPa<$d\omega/dP$<30.0 GPa	$d\omega/dP$>30.0 GPa
LO	251.6	4.65 ± 0.05	–	–
TO	204.9	5.69 ± 0.07	3.55 ± 0.51	–
TO splitting	180.9	−2.87 ± 0.09	6.95 ± 0.33	0.15 ± 0.07
New mode	351.2	–	–	1.91 ± 0.06

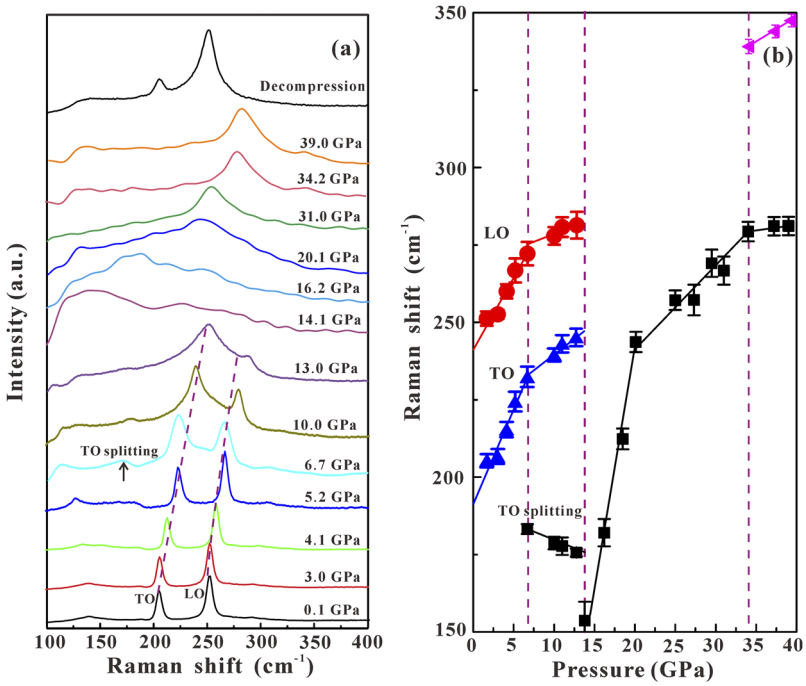

FIG. 2. (a) Raman spectra of ZnSe at the pressure range of 0.1–39.0 GPa and room temperature under the hydrostatic condition. (b) Raman shift of ZnSe with increasing pressure. TO: transverse optical mode and LO: longitudinal optical mode.

In terms of the phase transformations of ZnSe, previously reported Raman scattering results have been inconsistent. Some researchers suggest a structural phase transition of ZnSe from ZB to the cinnabar phase at ~5.0 GPa on the basis of one obvious splitting of the TO mode in Raman spectra under the hydrostatic condition.[7,8] On the contrary, another previous work did not observe any discontinuous variation in the slope of the pressure-dependent Raman shifts for 0–5.5 GPa, indicating that the zinc-blende phase of ZnSe is stable at this pressure range.[9] Considering the change from one individual peak to two independent new peaks in the splitting process of the TO mode observed in the Raman spectra herein, we determined the occurrence of a phase transition from ZB to the cinnabar structure for ZnSe at ~4.9 GPa under the non-hydrostatic condition. Additionally, the appearance of one obviously new peak at ~30.0 GPa has been ignored in previous Raman spectroscopy reports. This new peak may be attributed to a transition from the RS to Cmcm structure of ZnSe, as pointed out by previous reports using angle-dispersive diffraction and theoretical calculations.[15,16,21] Our Raman spectroscopy results provide robust evidence for a series of phase transformations of ZnSe from the zinc-blende to cinnabar to rock-salt to orthorhombic structure under both non-hydrostatic and hydrostatic conditions. The pressures of transformation from ZB-cinnabar-RS-Cmcm (6.7, 14.1 and 34.2 GPa, respectively) of ZnSe under the hydrostatic condition were delayed by more than ~2 GPa as compared to the pressures of transformation points (4.9, 12.5 and 30.0 GPa, respectively) under the non-hydrostatic condition. Moreover, as shown in Fig. 1, the variations in the Raman spectra upon decompression from 40.0 GPa were irreversible under the non-hydrostatic condition, though, one reversible characteristic was observed upon decompression under the hydrostatic condition. This may be attributed to the fact that high pressure is necessary to break the phase stability of the lattice structure, which will restrain the recovery of the lattice crystalline phase and result in an irreversible phase transition. In the present study, however, helium was used as a pressure medium that alleviated interlayer interactions owing to infiltration of the medium into the interlayer space at high pressure, which played a role in protecting the crystalline structure. The maximum value of ~40.0 GPa was not

TABLE II. Pressure dependence of the Raman shifts for ZnSe under the hydrostatic condition. The values of mode frequencies ω (P_0) (cm^{-1}), pressure P (GPa), and pressure dependence $d\omega_i/dP$ ($cm^{-1}GPa^{-1}$) were extrapolated. TO: transverse optical mode and LO: longitudinal optical mode.

Mode	ω (P_0)	$d\omega/dP$<6.7 GPa	6.7 GPa<$d\omega/dP$<14.1 GPa	14.1 GPa<$d\omega/dP$<34.2 GPa	$d\omega/dP$>34.2 GPa
LO	251.6	4.60 ± 0.12	2.42 ± 0.07	–	–
TO	204.7	4.27 ± 0.31	3.11 ± 0.02	–	–
TO splitting	182.2	–	−1.18 ± 0.01	5.83 ± 0.68	0.37 ± 0.05
New mode	340.8	–	–	–	0.17 ± 0.08

sufficiently high to completely destroy the original crystalline structure, and therefore our obtained Raman spectrum of ZnSe was recoverable after decompression under the hydrostatic condition, implying that this high-pressure phase transition is also reversible.

To confirm the pressure-induced variations in the crystalline and electronic structures, high pressure electrical conductivity measurements of ZnSe were carried out at pressures up to ~24.0 GPa at room temperature. Representative impedance spectroscopy for ZnSe at ambient temperature is given in Figs. 3(a)–(c) at various pressures up to ~24.0 GPa. At the pressure range 0.3–12.6 GPa, the impedance spectroscopy exhibits one approximately semicircular arc at high frequencies and a line at low frequencies, which respectively indicate the grain interior and grain boundary contribution. Initially, the semicircular arcs decreased with pressure, and then for pressures greater than ~4.4 GPa the semicircular arcs increased as the pressure increased to 12.6 GPa. The equivalent circuit of Figs. 3(a) and 3(b) contains two units, composed of R_{gi}–CPE_{gi} and R_{gb}–CPE_{gb} in series, where R and CPE represent the resistance and constant phase element, respectively; and the subscripts gi and gb denote grain interior and grain boundary, respectively. To verify deviation from the equivalent circuit, a typical impedance spectroscopy and its corresponding fitting curve at 0.3 GPa are shown in Fig. 3(b). Figure 3(c) shows the impedance spectroscopy as the pressure increases from 13.8 GPa to 24.0 GPa, which is only displayed in the fourth quadrant. The equivalent circuit of Fig. 3(c) was taken as a simple resistance. The obvious variation in the impedance spectroscopy indicated that the electronic crystal structure of ZnSe changed significantly at the pressure range 12.6–24.0 GPa, demonstrating pressure-induced electronic polarization.[18]

Figure 3(d) plots the pressure-dependent logarithm of the electrical conductivity of ZnSe in the process of compression at room temperature under the non-hydrostatic condition. Two obvious discontinuous points are observed at 4.4 and 13.8 GPa, which both exhibit an abnormal increase of electrical conductivity of the ZnSe sample that otherwise exhibits a decrease with increasing pressure. Further, at pressures greater than 13.8 GPa, the electrical conductivity becomes stable. These two obvious inflexion points are consistent with our Raman spectroscopy results and may be attributed to phase transitions. Additionally, the electrical conductivity is irreversible upon decompression under the non-hydrostatic condition. This obvious change in the electronic crystalline structure indicates that the ZnSe may undergo metallization.

To verify whether ZnSe undergoes pressure-induced metallization, we conducted a series of high-pressure

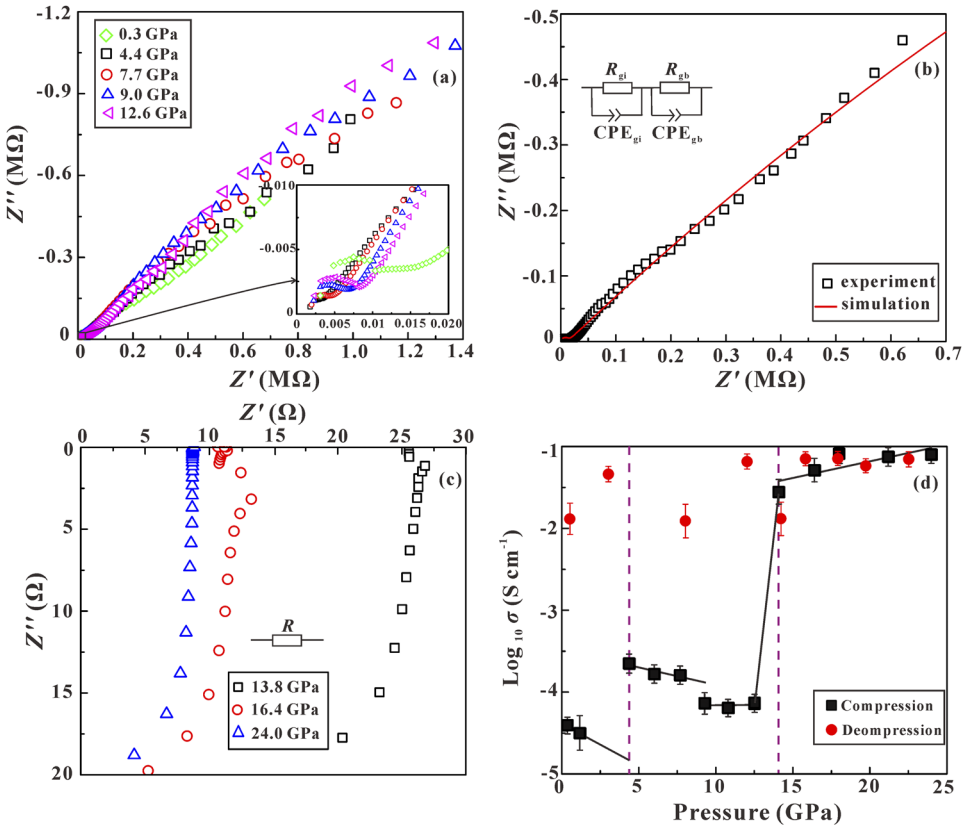

FIG. 3. (a) and (c) Selected impedance spectroscopy of ZnSe at the pressure range of 0.3–24.0 GPa and ambient temperature. (b) A typical fitted impedance spectroscopy of ZnSe using the equivalent circuit at 0.3 GPa and (d) pressure dependence of logarithm of electrical conductivity of ZnSe. *R*–resistance; CPE–constant phase element; gi–grain interior and gb–grain boundary.

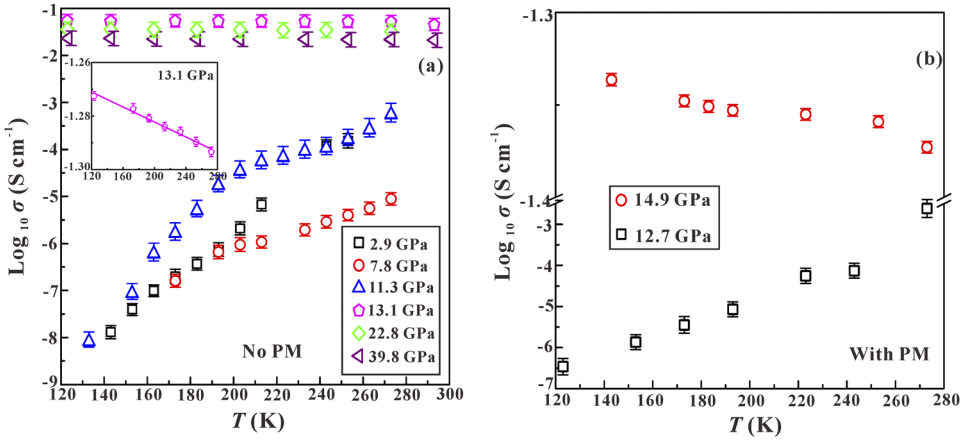

FIG. 4. (a) The temperature–dependent logarithm of electrical conductivity of ZnSe with pressure under the non–hydrostatic condition at the pressure range of 2.9–39.8 GPa and 123–293 K. (b) The temperature–dependent logarithm of electrical conductivity of ZnSe with pressure under the hydrostatic condition at 12.7 and 14.9 GPa and 123–273 K. PM: pressure medium.

variable–temperature conductivity measurements at pressures up to ~39.8 GPa and temperatures 123–293 K under non–hydrostatic and hydrostatic conditions. The relationship between electrical conductivity and temperature for ZnSe was found to satisfy the Arrhenius relation, as shown in Fig. 4. Under the non–hydrostatic condition, the electrical conductivity of ZnSe increased with increasing temperature at pressures less than 13.1 GPa, which is a typical semiconductor behavior. At the pressure range 13.1–39.8 GPa, the electrical conductivity decreased with temperature, which is a clear indication of pressure–induced metallization (Fig. 4(a)). Furthermore, the relationship of the logarithm of the electrical conductivity and the temperature under the hydrostatic condition given in Fig. 4(b) shows an increase in ZnSe electrical conductivity with increasing temperature for pressures less than 12.7 GPa, which is a typical semiconductor attribute. In contrast, the electrical conductivity decreased with increasing temperature at a pressure of 14.9 GPa, displaying a typical behavior of a metal. All of these results clearly indicated the occurrence of a pressure–induced metallization of ZnSe at ~13.1 under the non–hydrostatic condition and ~14.9 GPa under the hydrostatic condition.

Our obtained electrical conductivity results disclosed two ZnSe phase transitions at ~4.4 and ~13.1 GPa under the non–hydrostatic condition, which coincide well with our Raman scattering results. More specifically, the abnormal increase in electrical conductivity at ~4.4 GPa provides further robust evidence of the occurrence of a phase transition of ZnSe from ZB to the cinnabar structure. Further, the semiconductor–metal transformation of ZnSe at ~13.1 GPa is correspondent to the cinnabar–RS phase transformation. Therefore, we deduce that the subtle variation of the crystalline structure of the ZnSe sample is consistent with the transformed dielectric properties. In addition, the high–pressure variable–temperature conductivity results indicated that the metallization behavior of the ZnSe exhibited a significant dependence on the pressure environments. Under the non–hydrostatic condition, the metallization of ZnSe occurred at 13.1 GPa, while the transition point was increased ~2 GPa under the hydrostatic condition. This discrepancy in metallization phenomenon under different pressure environments can also be attributed to the effect that the pressure medium has in alleviating interlayer interaction. This protection that the pressure medium affords may mitigate the degree of destruction induced by the compression on the original crystalline structure, and further affect the occurrence of a structural phase transition. This crucial role of the pressure medium on the electrical properties of semiconductor material has also been confirmed by Zhuang *et al.*[17] On the basis of our Raman scattering and electrical measurements, the ZnSe may undergo structural phase transformations from ZB–cinnabar–RS structure at the respective pressures of ~4.9 and ~12.5 GPa, and then to a Cmcm phase at ~30.0 GPa under the non–hydrostatic condition.

In addition, in order to further explore the influence of the pressure medium, microstructural observations using high–resolution transmission electron microscopy were obtained of the recovered ZnSe under the non–hydrostatic and hydrostatic conditions. From Fig. 5(a), the original interlayer spacing of ZnSe for the (111) plane is found to be ~0.34 nm, which is in good agreement with the results of a previous study.[22] At the same time, the selected area electron diffraction pattern (SAED) of the initial powder sample could be nicely indexed to a ZB structure with the space group F–43m (PDF card No. 37–1463). After decompression from 39.0 GPa, the crystalline structure of the ZnSe was perfectly preserved under the hydrostatic condition, and we can roughly estimate an interlayer spacing of ~0.32 nm. The recovered layered crystalline structure was confirmed again by the corresponding SAED, as shown in (Fig. 5(b)). However, the SAED pattern became indistinct after decompression from 40.0 GPa under the non–hydrostatic condition, indicating a distortion in the crystalline structure for ZnSe (Fig. 5(c)). The existence of two phases can be clearly seen, where one phase possesses a layered crystalline structure and the other phase tends to be amorphous. Further, the interlayer spacing was calculated as ~0.25 nm. It was deduced that the sample was partially destroyed upon decompression from 40.0 GPa under the non–hydrostatic condition. The HRTEM images provide robust evidence that the reversibility of the crystalline structure under the hydrostatic condition was owing to the

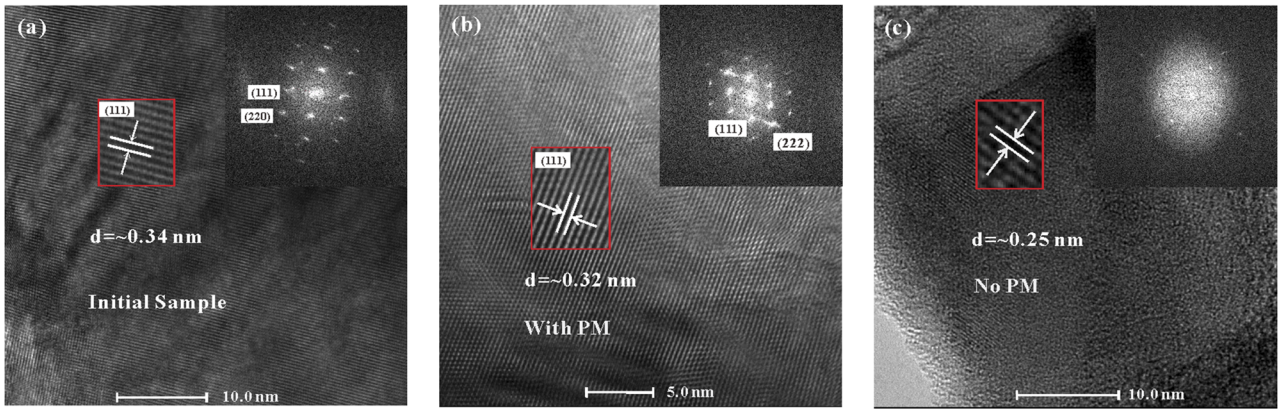

FIG. 5. HRTEM images of (a) initial ZnSe and (b and c) recovered samples from 39.0 and 40.0 GPa under the hydrostatic and non–hydrostatic conditions, respectively. Inset: representative selected area electron diffraction patterns by HRTEM. PM: pressure medium.

infiltration of helium atoms into the interlayer space. The pressure medium could thus weaken the interlayer interactions and allow the layered ZnSe structure to be reversible. All of the results obtained from the electrical conductivity measurements, Raman spectroscopy and HRTEM images revealed a unique high pressure behavior of ZnSe wherein the pressure environment exerts an obvious influence on the crystalline structure.

IV. CONCLUSIONS

In the present study, the structural, vibrational and electrical properties of ZnSe under different pressure environments in a DAC up to ~40.0 GPa and at temperatures ranging from 123–293 K were systematically investigated using ac impedance spectroscopy, Raman spectra and HRTEM. Our obtained Raman scattering and electrical conductivity results showed a ZnSe transformation from a ZB to a cinnabar phase at ~4.9 GPa under the non–hydrostatic condition. A semiconductor–metal transformation was determined at ~12.5 GPa on the basis of the disappearance of LO mode in Raman spectroscopy and temperature–dependent conductivity measurements. Additionally, by virtue of the appearance of a new peak in the Raman spectrum, another phase transition for ZnSe from RS to Cmcm was determined to exist at ~30.0 GPa. It was found that the structural phase transitions of ZnSe were irreversible under the non–hydrostatic condition. Under the hydrostatic condition, however, the transformations of ZnSe were delayed and reversible, where the transition pressures of ZB–cinnabar–RS–Cmcm were determined as 6.7, 14.1 and 34.2 GPa, respectively. In this regard, we emphasize that the pressure medium can mitigate the interlayer interactions of ZnSe.

ACKNOWLEDGMENTS

This research was financially supported by the Strategic Priority Research Program (B) of the Chinese Academy of Sciences (XDB 18010401), Key Research Program of Frontier Sciences of CAS (QYZDB-SSW-DQC009), "135" Program of the Institute of Geochemistry of CAS, Hundred Talents Program of CAS and NSF of China (41474078, 41774099 and 41772042).

REFERENCES

[1] G. A. Samara and H. G. Drickamer, J. Phys. Chem. Solids **23**, 457 (1962).
[2] C. H. Bates, W. B. White, and R. Roy, Science **137**, 993 (1962).
[3] P. J. Smith and J. E. Martin, Phys. Lett. **19**, 541 (1965).
[4] S. K. Gupta, S. Kumar, and S. Auluck, Physica B **404**, 3789 (2009).
[5] B. A. Weinstein, Solid State Commun **24**, 595 (1977).
[6] M. A. Haase, J. Qiu, J. M. Depuydt, and H. Cheng, Appl. Phys. Lett. **59**, 1272 (1991).
[7] C. M. Lin, D. S. Chuu, T. J. Yang, W. C. Chou, J. A. Xu, and E. Huang, Phys. Rev. B **55**, 13641 (1997).
[8] L. D. Yao, F. F. Wang, X. Shen, S. J. You, L. X. Yang, S. Jiang, Y. C. Li, K. Zhu, Y. L. Liu, A. L. Pan, B. S. Zou, C. W. Jin, and R. C. Yu, J. Alloys Compd. **480**, 798 (2009).
[9] A. K. Arora, E. K. Suh, U. Debsks, and A. K. Ramdas, Phys. Rev. B **37**, 2927 (1988).
[10] R. G. Greene, H. Luo, and A. L. Ruoff, J. Phys. Chem. Solids **56**, 521 (1995).
[11] G. Itkin, G. R. Hearne, E. Sterer, M. P. Pasternal, and W. Potzel, Phys. Rev. B **51**, 3795 (1995).
[12] H. Karzel, W. Potzel, M. Kofferlein, W. Schiessl, M. Steiner, U. Hiller, and G. M. Kalvius, Phys. Rev. B **53**, 11425 (1996).
[13] S. V. Ovsyannikov, V. Vladimir, V. V. Shchennikov, A. Misiuk, and I. A. Komarovsky, Phys. Status Solidi B **246**, 604 (2009).
[14] M. Durandurdu, J. Phys: Condens. Mater. **21**, 125403 (2009).
[15] M. Cote, O. Zakharov, A. Rubio, and M. Cohen, Phys. Rev. B **55**, 13025 (1996).
[16] S. X. Cui, H. Q. Hu, W. X. Feng, X. S. Chen, and Z. B. Feng, J. Alloys Compd. **472**, 294 (2009).
[17] Y. K. Zhuang, L. D. Dai, L. Wu, H. P. Li, H. Y. Hu, K. X. Liu, L. F. Yang, and C. Pu, Appl. Phys. Lett. **110**, 122103 (2017).
[18] L. D. Dai, Y. K. Zhuang, H. P. Li, L. Wu, H. Y. Hu, K. X. Liu, L. F. Yang, and C. Pu, J. Mater. Chem. C **5**, 12157 (2017).
[19] L. D. Dai, K. X. Liu, H. P. Li, L. Wu, H. Y. Hu, Y. K. Zhuang, L. F. Yang, C. Pu, and P. F. Liu, Phys. Rev. B **97**, 2 (2018).
[20] S. S. Mitra and O. Brafman, Phys. Rev. B **186**, 942 (1969).
[21] M. I. Mcmahon and R. J. Nelmes, Phys. Status Solidi B **198**, 389 (1996).
[22] S. V. Pol, V. G. Pol, J. M. Calderon-Moreno, S. Cheylan, and A. Gedanken, Langmuir **24**, 10462 (2008).